

The Fourier Kelvin Stellar Interferometer (FKSI): A review, progress report, and update

W. C. Danchi^{*a}, R. K. Barry^a, P. R. Lawson^b, W. A. Traub^b, S. Unwin^b

^aNASA Goddard Space Flight Center, Code 667, Greenbelt, MD 20771 USA;

^bJet Propulsion Laboratory, California Institute of Technology, Pasadena, CA 91109

ABSTRACT

The Fourier-Kelvin Stellar Interferometer (FKSI) mission is a two-telescope infrared space interferometer with a 12.5 meter baseline on a boom, operating in the spectral range 3 to 8 (or 10) microns, and passively cooled to about 60 K. The main goals for the mission are the measurement and characterization of the exozodiacal emission around nearby stars, debris disks, and the atmospheres of known exoplanets, and the search for Super Earths around nearby stars. We discuss progress on this mission in the context of the upcoming Decadal Survey, in particular how FKSI is ideally suited to be an Exoplanet Probe mission in terms of crucial observations which should be done before a flagship mission can be undertaken, as well as technical readiness, cost, and risk.

Keywords: Protoplanetary Disks, Debris Disks, Exozodis, Exoplanets, Nulling Interferometry, Infrared Techniques, Passive Cooling, Infrared Detectors, Cryomechanisms, Infrared Optics, Cold Optics

1. INTRODUCTION

The long-term focus of planet finding efforts at NASA has been directed towards the search for extrasolar terrestrial planets, like those in our own solar system, within the habitable zone around stars similar to our own Sun, e.g., F, G, and K main sequence stars. Our present theoretical understanding is that all planets form out of material in primordial disks from which the stars themselves accreted material. Thus, the formation of planets is intimately linked to the evolution of circumstellar disks.

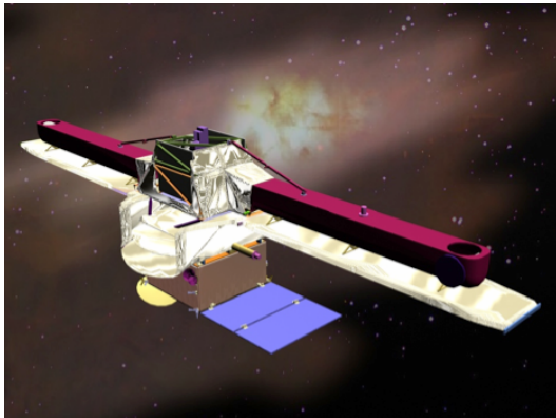


Figure 1. Artist's conception of a sample small prototype planet finding mission, that of the FKSI mission concept, which has been extensively studied.

material has been observed, but upper limits correspond to the equivalent of the emission of 1500 times that of our Solar System Zodiacal (SSZ) light.

Over the past 13 years, about 300 extrasolar planets have been discovered using precision radial velocity techniques (Mayor & Queloz 1995, Marcy & Butler 1998), transit searches (Charbonneau et al. 1999, Alonso et al. 2004), microlensing (Bennett et al. 1999), imaging (Chauvin et al. 2005), and pulsar timing (Wolszczan et al. 1992). A summary of data on known exoplanets is available in Schneider (2008). The lower limit of detectable masses has decreased from about 100 Earth masses (M_E) to about 4 M_E .

In the past five years infrared emission has been observed from circumstellar disks that are remnants of the primordial disks. For example, the Spitzer Space Telescope primarily observed cool material at 24 and 70 μm , corresponding to distances of 5-10 AU or greater from the parent stars (Bryden et al. 2006, Beichman et al. 2005), while studies with SCUBA at the JCMT observe even cooler material, out to 100 AU (Greaves et al. 1998, Holland et al. 1998). On some systems, warmer

*Contact information: NASA Goddard Space Flight Center, Exoplanets and Stellar Astrophysics, Code 667, Greenbelt, MD 20771 USA, e-mail: william.c.danchi@nasa.gov, phone: 1 301 286 4586, fax: 1 301 286 1753

Advanced Imaging in the Mid-Infrared: Planetary Formation, Debris and Exozodiacal Disks, and Direct Detection of Exoplanets

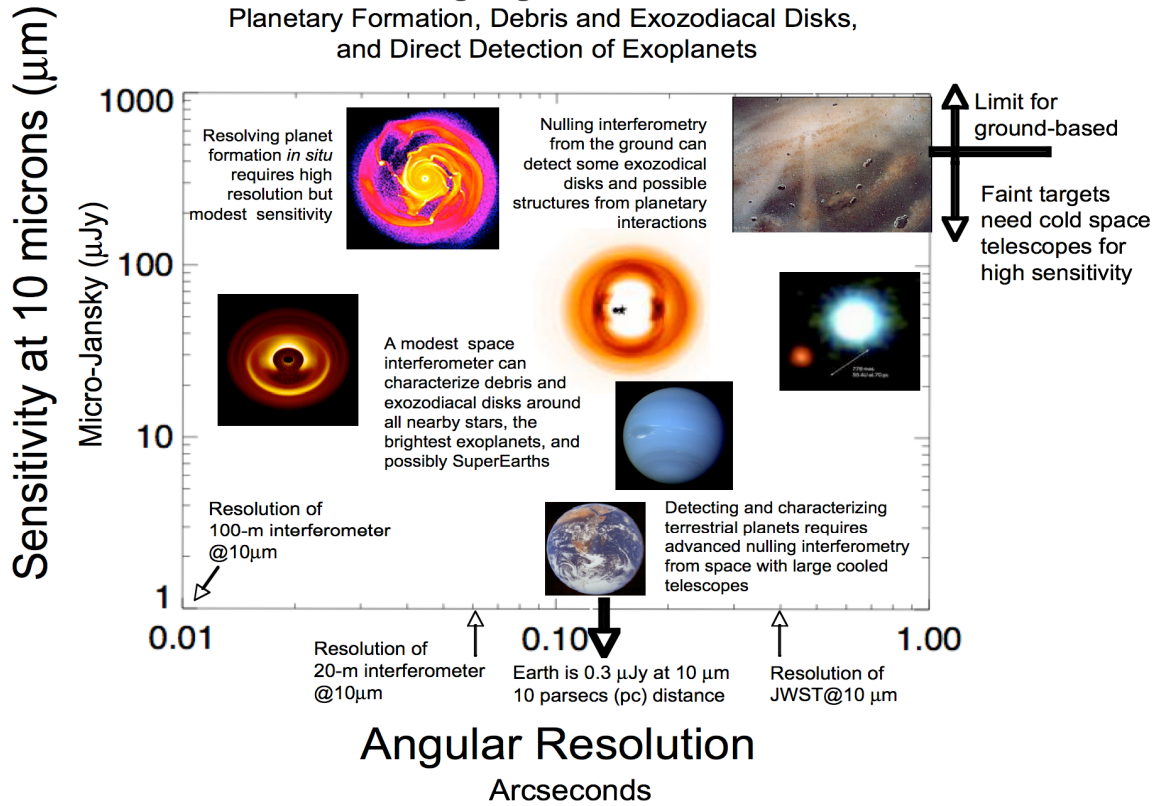


Figure 2. Relationship between resolution and sensitivity for advanced imaging in the infrared for planet formation, debris and exozodiacal disks, and direct detection of exoplanets.

Recent studies of the requirements for planet finding and characterization missions such as the Terrestrial Planet Finder (TPF) have shown that the amount of exozodiacal emission from warm and hot dust in the habitable zone is a crucial parameter. Observations of planets in stellar systems with more than about 10 SSZs will be extremely difficult as exozodiacal dust emission (and/or scattering) interferes with the observer's ability to detect the faint emission from an Earth-like planet. Thus it is crucial to observe all of the likely targets for TPF to determine the amount of exozodiacal emission around nearby stars with sufficient accuracy for the flagship missions. In particular we must answer the question, "What is the star-to-star statistical distribution of exozodiacal material in the habitable zone around nearby stars?" The need for this measurement is documented in the report from the ExoPlanetary Task Force (Lunine et al. 2008).

This measurement can be made with a small infrared interferometer having apertures ~0.5-1 m in diameter and which is passively cooled to about 60 K. One such implementation, called the Fourier-Kelvin Stellar Interferometer (FKSI), shown in the artist's conception of Figure 1, (Danchi et al. 2003a), has been under development since 2002 (Danchi et al. 2002). A substantial number of papers have been written describing this mission concept (Barry et al., 2008; Defrere et al., 2008; Danchi & Lopez, 2007; Danchi et al., 2006; Frey et al., 2006; Barry et al., 2006a; Barry et al., 2006b; Richardson et al., 2006) and are available from the Astronomical Data Service (ADS) or from the authors of this paper.

The larger context of this mission concept is that of technical progress in resolution and sensitivity in the near- and mid-infrared, which is shown in Figure 2. This diagram displays resolution from 10 milli-arcseconds (mas) to 1 arcsec on the horizontal axis and the required sensitivity in Janskys ($10^{-26} \text{ W m}^{-2} \text{ Hz}^{-1}$) on the vertical axis. Ground-based systems can have high angular resolution, such as that of the Keck Interferometer with its 85 m baseline, which has an angular resolution ($\lambda/2B$) of ~12 mas at 10 microns, but sensitivity limited to ~1 Jy. Cooled space based filled

aperture telescopes such as Spitzer and JWST have resolutions ($1.22 \lambda/D$) of ~ 3 arcsec and ~ 0.4 arcsec, respectively at 10 microns. Cooled formation-flying interferometers, such as TPF-I and Darwin, fit into the lower left corner of the diagram, which is the ultimate goal for research in this wavelength region. However, studies of the last five years have shown that these projects, while technically feasible, are unlikely to be within any foreseen cost envelopes for either NASA or ESA until the 2020+ time frame. Fortunately a middle ground exists, where a modest-sized structurally connected interferometer, such as the FKSI mission concept has a substantially discovery space for transformative science in star and planet formation, evolution of planetary disks, debris disks, exozodi levels around nearby stars, and characterization of the atmospheres of known exoplanets and super-earths.

The focus of this paper will be to highlight the current status of observations in two key science areas of the FKSI mission concept, and to show how this mission will transform our knowledge and prepare for future flagship missions. In addition we review the implementation of the concept, as well as cost and technological readiness. Finally we describe some useful cost and science return trades that would be of benefit to the project as the US community prepares for the Decadal Survey and the Exoplanet Probe Announcement of Opportunity (AO) expected in the near term.

2. SCIENTIFIC CONTEXT

2.1 Debris Disks

2.1.1 Observational Progress on Debris Disks

During the past five years, observers using the Spitzer Space Telescope and the James Clerk Maxwell Telescope have made progress on studies of the frequency of debris disks around solar type stars, and the characteristics of debris disks previously discovered by IRAS (Auman et al. 1984, Plets & Vynckier 1999) and ISO (Spangler et al. 2001). The major focus of these studies has been on the decay of planetary debris disks (e.g., Rieke et al. 2005) and on the frequency of such disks around solar type stars (Bryden et al. 2006, Beichman et al. 2005, Kim et al. 2005). Debris disks have been discovered around stars having a range of masses from A to K stars (e.g. Beichman et al. 2005), and white dwarf stars (Reach et al. 2005).

Spitzer MIPS observations at $70 \mu\text{m}$ (Beichman et al. 2005) found that there were 6 of 26 main sequence stars (with radial velocity detected planets) with substantial debris disks, and hence that excess emission was as common around the main sequence stars as in earlier observations of A and F stars with IRAS. Spitzer observations also improved the detection threshold, $L_{\text{dust}}/L_{\text{star}}$, from $\sim 10^{-3}$ with IRAS to $\sim 10^{-5}$ (Kim et al. 2005).

The morphology of debris disks has been investigated around a number of stars, including ϵ Eri, β Pic, Fomalhaut, and Vega (Holland et al. 1998, 2003) at 450 and $850 \mu\text{m}$, and HR 4796A (Koerner et al. 1998, Jayawardhana et al. 1998) at 10 and $20 \mu\text{m}$. These observations show a number of complex features, such as cavities, asymmetries, and clumps, which could be due to the resonant trapping of dust associated with a large planet, and other important dynamical phenomena such as collisional cascades of dust from interactions between planetesimals, and the interplay with effects like radiation pressure and Poynting-Robertson and gas collisional drag.

These studies have focused on the cold outer regions of the debris disk systems, where the dust temperatures are around 50 K, which is a different population of dust than is most important for the search for earth-like planets in the habitable zone, where the dust should be around 300 K. Present limits are several orders of magnitude greater than expected for the hotter material in our own zodiacal cloud (Dermott et al. 2002), which is about $L_{\text{dust}}/L_{\text{star}} \sim 10^{-7} - 10^{-8}$. Cooler material in our Kuiper belts is predicted to be of the order of $10^{-6} - 10^{-7}$ (Stern 1996).

2.1.2 Debris Disk Parameter Space to be Explored with FKSI

Spitzer observations (also Herschel and JWST) measure dust excesses relative to the stellar spectrum, which is extrapolated to the infrared. Calibration uncertainties limit the excesses measured to a few percent over that of the estimated stellar spectrum. This gives the limit to Spitzer observations of ~ 1000 SSZs. Current observations are most sensitive at the longer wavelengths, namely, $70 \mu\text{m}$ for Spitzer and in the submillimeter for the SCUBA observations at JCMT. Thus present observations constrain extrasolar zodiacal emission from the population of dust associated with distances of 10 AU and greater, which may have very different characteristics than the population of dust at 1 AU in the habitable zone, of most interest to TPF and Darwin.

Ground-based nulling interferometers, such as the Keck Interferometer Nuller and the nulling instrument on the Large Binocular Telescope Interferometer (LBTI), can make significant progress on this latter population of dust since they will observe at $10 \mu\text{m}$ near the peak of the 300 K blackbody emission. However, our present understanding of the limitations of ground-based warm nulling systems is that they will push the limit to 30-100 SSZs around nearby stars,

still far larger than is needed for sizing the TPF and Darwin missions. The reason ground based nulling interferometers can make additional progress is that they suppress the star light and enable a clearer distinction between stellar and zodiacal light, thus bypassing the limitations of a purely spectroscopic approach.

Another limitation to purely photometric or spectroscopic studies is the lack of spatial resolution. This is especially significant as clumps and asymmetries in the distribution of debris disk material can be used to search for unseen planets. Thus, it is vitally important to know that the emission is coming from the region of the habitable zone, and to know the amount of dust for the TPF target stars. It is unlikely that we can know for certain what are the best TPF target stars (from the standpoint of exozodiacal dust) without a mission that provides this essential information.

FKSI uniquely provides the capability to bypass these limitations. The combination of null depth (contrast), sensitivity, and spatial resolution will allow for the first high-sensitivity measurement of zodiacal dust emission in the habitable zone of all nearby stars.

2.2 Exoplanets

2.2.1 Some characteristics of known extrasolar planets.

The currently known exoplanets cover an impressively broad range of semi-major axes from about 0.02 AU up to about 6 AU and masses from about 10 M_J to about 0.015 M_J . These planets also cover a very wide range of eccentricities, which are quite different and distinct from our own Solar System.

Of the 307 planets, currently 52 are transiting planets, and for these much more physical knowledge can be gained since the inclination angle (i), the planet radius (R_p) and hence the mean density can be determined. Precision photometry has been used with the transiting planets to determine the temperature of the atmosphere [Deming et al. (2005, 2006), Charbonneau et al. (2005)], chemistry [Charbonneau et al. 2002, Vidjal-Madjar et al. 2003], and albedo [Rowe et al. 2006]. The first emission spectra of transiting planets was published by Richardson et al. (2007) for HD 209458b and Grillmair et al. (2007) for HD 189733b, using secondary transits observed with the Spitzer Space Telescope.

While detection of new extrasolar planets will continue, the importance of the physical characteristics of known planets becomes increasingly clear. The diversity of exoplanetary systems provides a unique laboratory to study the formation, dynamics, and evolution of planetary systems. This will allow us to place our own Solar System and those like our own in the larger context of stellar and planetary origin and evolution.

Figure 3(a) displays a table of planetary characteristics that can be determined using FKSI, including planetary temperature, radius, mass density, albedo, surface gravity, and atmospheric composition, including the presence of water. To date, progress has been made on the physical characteristics of planets largely through transiting systems, however FKSI can measure the emission spectra of a large number of non-transiting ones.

Orbital Parameters	What FKSI does:
Removes $\sin(i)$ ambiguity	Measure
Planet Characteristics	
Temperature	Measure
Temperature variability due to distance changes	Measure
Planet radius	Measure
Planet mass	Estimate
Planet albedo	Cooperative
Surface gravity	Cooperative
Atmospheric and surface composition	Measure
Time variability of composition	Measure
Presence of water	Measure
Solar System Characteristics	
Influence of other planets, orbit coplanarity	Estimate
Comets, asteroids, zodiacal dust	Measure

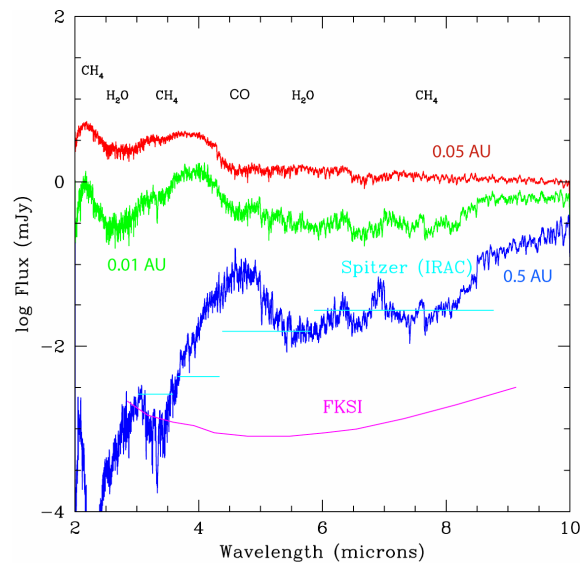


Figure 3. (a) Left panel. Characteristics of exoplanets that can be measured using FKSI. The term Cooperative indicates that these characteristics may be derived through combination of data from FKSI and other existing instruments. (b) Right panel. The FKSI system can measure the spectra of exoplanets with a wide range of semi-major axes.

2.2.2 Exoplanet parameter space to be explored with the FKSI system.

Transit observations of exoplanets have dramatically deepened our knowledge of their physical parameters. Transit light curves have been used to determine the radius and inclination angle of exoplanets to high precision, in turn leading to the measurement of mean density. Most exoplanets have densities close to 1 g cm^{-3} , the density of water; this is significantly below the $\sim 5 \text{ g cm}^{-3}$ typical of “rocky” planets such as Earth.

Many molecular species, such as carbon monoxide, methane, and water vapor, have strong spectral features in the 3-8 μm region, as can be seen in Figure 3(b), which displays model atmospheres for extrasolar planets calculated by Seager (2005), for planets at various distances from the host star. The red curve shows the theoretical spectrum of a very hot, close-in planet at 0.05 AU, while the blue curve displays spectrum for a much cooler planet ten times further out, at 0.5 AU. Also displayed are sensitivity curves for the IRAC instrument on Spitzer (light blue) and FKSI (purple). Clearly the FKSI mission concept (with nominal characteristics described in Fig. 3) has sufficient sensitivity to detect and characterize a broad range of extrasolar planets.

In addition to observations of the atmospheres of giant planets, FKSI can contribute to understanding the typical distribution of giant planets in wide orbits ($>5\text{-}10 \text{ AU}$). Such planets can dominate the dynamical environment of the habitable zone, and affect the delivery of volatiles to terrestrial planets (Lunine 2001). Planets on eccentric orbits may disrupt the habitable zone or affect the composition by perturbation of outer planetesimals into crossing orbits with the habitable zone. Understanding the placement and orbital parameters of outer planets is an important prerequisite to searching for terrestrial planets in these systems. Such observations are difficult to obtain from ground-based telescopes. Massive or young planets can be detected (cf. Lafreniere et al. 2007, Hinz et al. 2006), but planets that are older than $\sim 0.5 \text{ Gyr}$ or are less massive than Jupiter are not detectable with 8 m class ground-based telescopes. FKSI can explore this parameter region and provide information that can, in a way similar to exozodiacal dust and debris disk characterization, identify star systems that can nurture Earth-like planets.

The apparently commonplace nature of lower mass planets suggests an intermediate class of planets may be observable with FKSI, the super-Earth. A prime example of this is the planetary system of GL 581. The outer two planets of this system are near the habitable zone of the star. Selsis et al. (2007) have analyzed this system and suggest the outer planet (planet d, $a=0.25 \text{ AU}$, $R\sim 2R_E$, $M\sim 8M_E$) is the most likely to be habitable. Since the star is at 6.3 pc, the planet's angular separation, 0.04 arcsec, is at the first maximum of the fringe pattern of FKSI. At four times the flux of an Earth-size planet, GL 581d would be within the sensitivity limit of the FKSI system. Thus there is already one known, possibly Earth-size planet that could be observed with FKSI. As more super-Earths are discovered, it is likely that FKSI will have at least a small sample of objects that might be characterized for the atmospheric constituents and could indicate habitability.

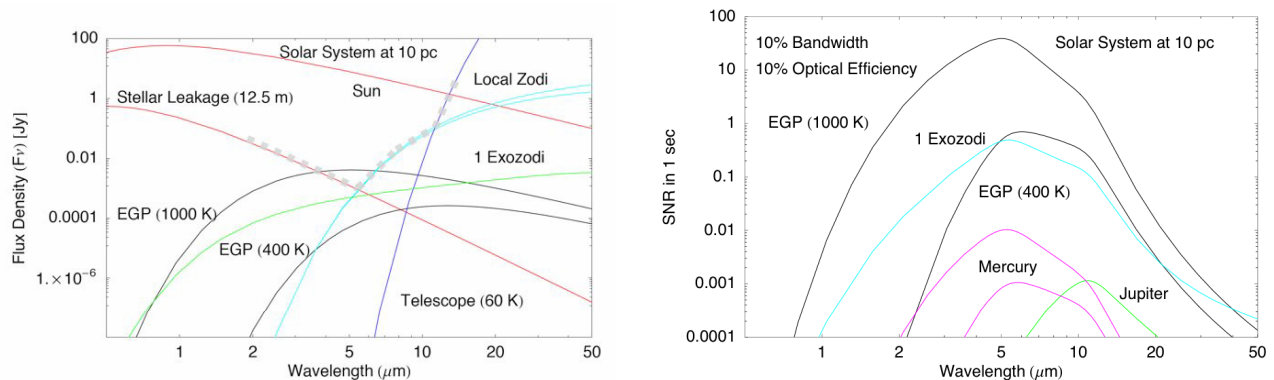


Figure 4. (a) Left panel. Flux density versus wavelength for a variety of sources affecting the performance of a cooled nulling space interferometer. The gray dashed line outlines the boundary created by the dominant noise sources: telescope emission, local zodiacal emission and stellar leakage (b) Right panel. Estimate of system performance (signal-to-noise ratio) for 1 m^2 collecting area, for 10% bandwidth and 10% optical efficiency.

3. TECHNIQUES AND REQUIRED CAPABILITIES

3.1 Nulling Interferometry is Interferometric Coronagraphy

The technique used to suppress starlight in order to achieve a high dynamic range in the infrared is nulling interferometry, which is the sparse aperture equivalent of optical coronagraphy employed on conventional (filled-aperture) telescopes. A “null” condition is created by a 180-degree reversal of the electric field from one of the two telescope apertures that are both pointed accurately at the same star. The electric fields are combined on dielectric beam splitters, producing a sinusoidal transmission pattern on the sky that looks somewhat like a picket fence, such that a vertical piece of the fence or dark stripe blocks the light from the star itself, while allowing the transmission of light from angles away from the star itself. Infrared radiation emitted from a planet or dust from a debris disk is transmitted and is detected on the null or dark port of the optical system. Interferometers are employed in the infrared because they can obtain the very high angular resolution ($\ll 1$ arcsec) that is required to detect and characterize exozodiacal debris and planets around nearby stars (see the paper by Barry et al. 2008, which describes the operation and data reduction for the Keck Interferometer Nuller).

Calculations of signal and noise sources affecting the detection and characterization of exoplanets in the 3-8 μm region of the spectrum are presented in Figure 4 (a), with expected signal levels in Jy ($10^{-26} \text{ W m}^{-2} \text{ Hz}^{-1}$) as a function of wavelength (μm) for our Sun and viewed from a reference distance of 10 pc. Flux density levels for extrasolar giant planets at 400 K and 1000 K, for an exoplanet with radius (1.35 R_J) and albedo of HD209458b are also shown. Figure 4(a) also displays expected noise sources including emission from the stellar leakage (due to the finite size of the star), emission from the exozodiacal dust cloud (based on the model of Reach et al. (2003)) from a dust cloud having the same characteristics as our own zodiacal cloud, emission from the local zodiacal cloud itself, and the thermal emission from the telescope system at 60 K. The gray dashed line outlines the boundary created by the dominant noise sources, from stellar leakage (short wavelengths), to the emission from the local zodiacal cloud (middle wavelengths), and the emission from the telescope itself (longest wavelengths), demonstrating the SNR is optimum in the 3-8 (or 10) μm region.

Figure 4(b) shows the expected signal to noise ratio in 1 s for a 1 m^2 mirror, assuming a 10% bandwidth, and 10% optical efficiency for an integration time of 1 second. Radii and albedos of the solar system planets were taken from the tables of Lissauer and DePater (2001). Clearly, warm and hot exo-Jupiters are easy to detect with this short integration time, as are exozodiacal clouds.

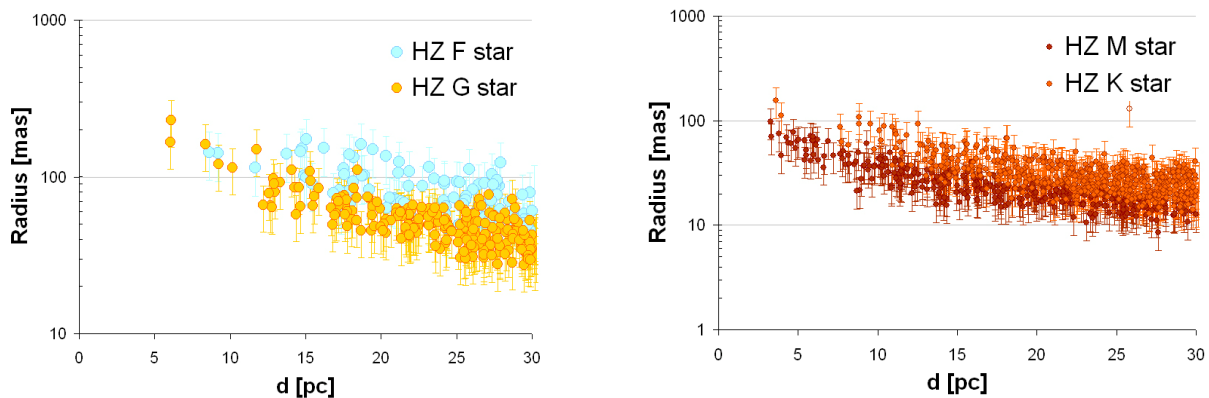


Figure 5. The extent of the Habitable Zone for the single main sequence stars (F,G stars on left panel, and M, K stars on right panel) within 30 pc from the Sun (from Kaltenegger et al 2008)

3.2 Angular resolution.

The angular scale of the planetary system determines the required resolution of an imaging system. At 10 pc, the Earth at 1 AU corresponds to an angular separation of ~ 0.1 arcsec, while Jupiter would be at about 0.5 arcsec. The inner working angle (IWA) of a nulling interferometer is equal to its angular resolution ($\lambda/2B$), thus with baseline, $B = 12.5$ m, at $\lambda = 5 \mu\text{m}$, the IWA of the FKSI is ~ 0.04 arcsec. A number of exoplanets have apparent separations resolvable with FKSI (cf. Figure 5), but planets with much smaller semi-major axes can also be detected and characterized using a two-color technique (Danchi et al. 2003a,b). As a comparison, coronagraphic observations on JWST have an inner

working angle (IWA) of $\sim 4 \lambda / D \sim 0.7$ arcsec at $\lambda=5 \mu\text{m}$ and $D=6$ m. This much larger IWA means that the JWST will be unable to probe the dust and planets in the region near the habitable zone for nearby stars, only zones corresponding to the outer planets and Kuiper belts. Figure 5 displays the angular separation of the habitable zone around nearby F and G stars (left panel) and M and K stars (right panel) as a function of distance to the Earth. Clearly the habitable zone is accessible for a large number of these stars even for interferometers with modest resolutions, of the order of 40 mas.

3.3 Spectral resolution.

The spectral resolution requirement depends on the width of the features that must be resolved. From Fig. 2(b), it is clear that a spectral resolution, $R \sim 25-50$, is adequate to resolve the molecular features in the planet's atmosphere. The lower limit for the spectral resolution is set by Nyquist sampling of the narrowest methane feature centered at $7.5 \mu\text{m}$. In addition to mass, the variation in the planet's infrared spectrum as a function of phase is necessary to characterize the planet's thermal state and composition. In favorable cases, inferences about dynamical properties of the atmospheres such as winds could be made (Showman & Guillot 2002). This approach of exploiting the infrared brightness of exoplanets builds on the transit and radial velocity studies.

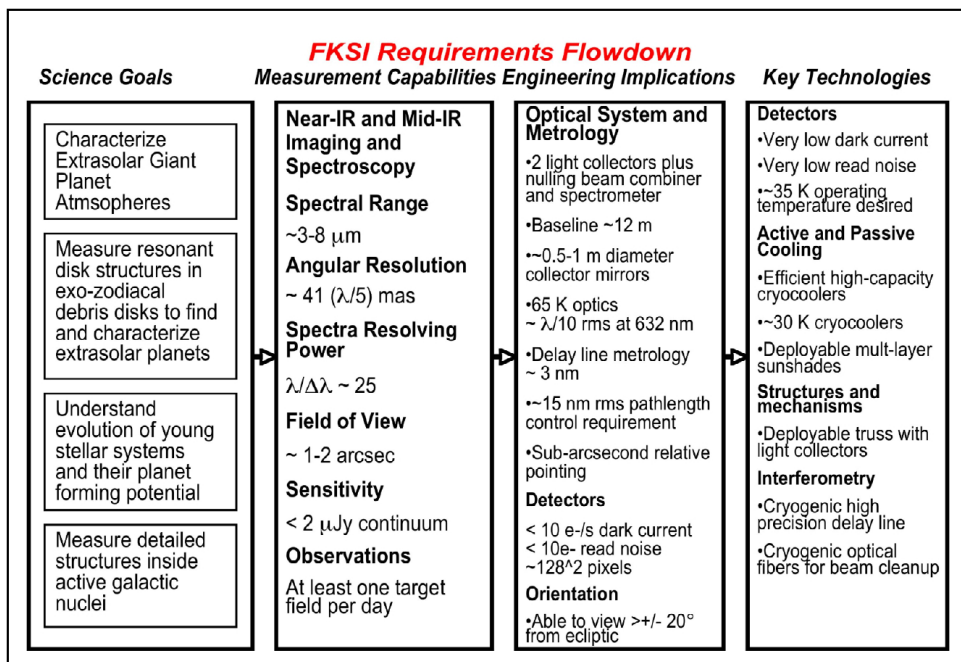


Figure 6. To obtain the performance characteristics needed to achieve the FKSI scientific goals, careful engineering and the continued development of a few technologies will be needed. Here we schematically demonstrate the requirements flowdown for FKSI.

3.4 Requirements flowdown

In order to determine the performance characteristics needed for this mission, we have performed a flowdown from the key science requirements to major instrumental performance requirements, as shown in Figure 6.

4. IMPLEMENTATION CONCEPT

The FKSI implementation is a two-telescope passively cooled nulling interferometer operating between 3 and 8 μm . The FKSI observatory will operate at the second Sun-Earth Lagrange point (L2) in a large amplitude Lissajous (or halo) orbit. While we have explored a range of aperture sizes for FKSI, our baseline design employs 0.5 m apertures. The telescopes employ two flat mirrors (siderostats) mounted 12.5-m apart on composite support booms, minimizing alignment requirements for the beams that enter the instrument package. The booms support sunshades that allow passive cooling of the structure to 60K, reducing thermal noise in the telescope system to a level that is negligible compared to that from the local zodiacal cloud (zodiacal background limited performance) over most of the instrument

passband. This design also allows for complete testing of the entire system in the large test chamber at Goddard Space Flight Center (GSFC) by mounting the siderostats on “stub” booms during the I&T phase. Also it is possible to install the entire FKSI system with the flight booms deployed into the large test chamber at Marshall Space Flight Center, if modifications were made to the cryogenic insert.

The mechanical design concept for the FKSI is shown in Fig. 7 and was derived over approximately one year of studies in 2002-2003 after initial work in GSFC’s Integrated Mission Design Center (IMDC) and Instrument Synthesis and Analysis Laboratory (ISAL). Three major designs were developed during the course of this work, with end product FKSI designs A, B, and C (Fig. 8). The goal at the time was to develop a practical and robust infrared space interferometer that could fit into a Discovery cost cap of that epoch. The result was a mission concept with relatively low complexity and risk, but that was approximately \$100 million over the cost cap at the time of the last Discovery AO. The present FKSI design underwent a thorough review by GSFC Center Management during that time period, and a complete design exists including preliminary designs for all the major optical and mechanical subsystems, as well as launch, deployment, and mission and science operations. Multiple detailed cost studies have been made to date, including grass roots, PRICE H parametric models, and a cost assessment performed by GSFC’s Resource Analyst Office (RAO).

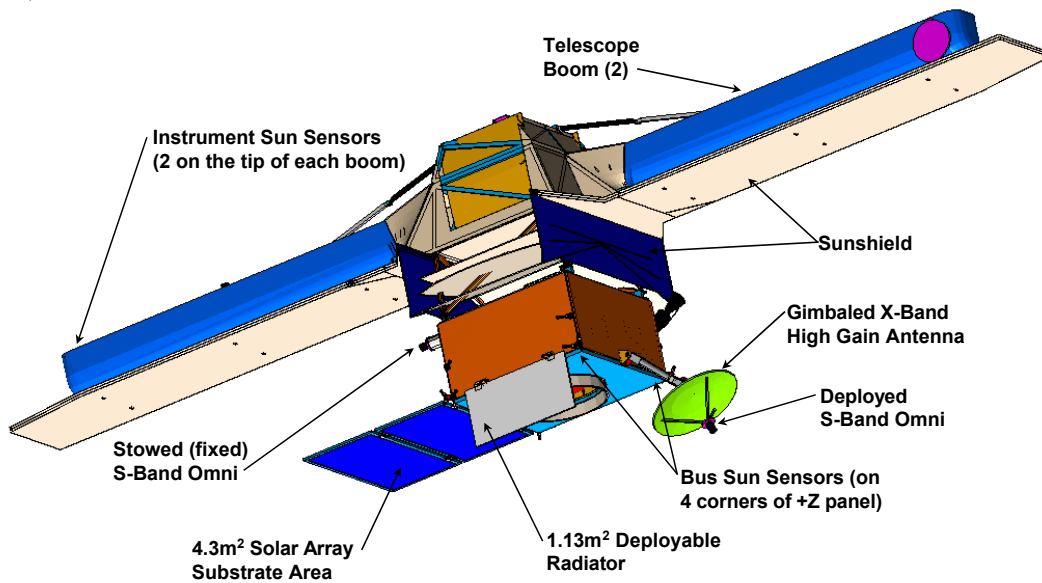


Figure 7. The FKSI mechanical design.

The mechanical design is appropriate for the payload attachment fitting (PAF) for the smallest of the Atlas V launch vehicles with a 4-m diameter fairing. The design minimizes the number of deployments. They are: (1) and (2) the two siderostats mounted on the ends of the booms, separated by 12.5 m, deployed using the well proven MILSTAR hinge technology. The booms are made from composite structures for an optimal strength to weight ratio, and the fixed sunshades are mounted to them; (3) a high-gain gimbaled S band antenna for the data downlink; (4) a solar array for power; and (5) a radiator. The dry mass of the bus was 805/1006 kg without/with contingency, and the propellant is hydrazine with a mass of 243 kg. The total dry spacecraft mass without/with contingency is 2352/2939 kg, for a total wet mass of 3183 kg at launch. The peak power is estimated to be ~750 W.

A schematic diagram of the optical design is shown in Fig. 9. There are five major subsystems in the instrument payload, which is mounted through a low mechanical frequency coupling and gamma-Al struts to the spacecraft bus. These include: (1) the boom-truss assembly which holds the siderostat mirrors and the non-deployed sunshields; (2) the main instrument module and optical bench assembly which includes a pair of off-axis parabolic mirrors for afocal beam size reduction, and also a fast steering mirror assembly for the control of fine pointing, two optical delay lines (one to be used, the other is a spare), and two dichroic beam splitters, one for the angle tracker and fringe tracker assemblies (0.8-2.5 μm), the other for the science band of 3-8 μm ; (3) the angle tracker assembly for fine pointing; (4) the fringe tracker assembly for stabilizing the fringes for the nulling instrument assembly; and (5) the nulling instrument assembly itself.

The nulling instrument is based on a modified Mach-Zehnder beamsplitter design that maximizes the symmetry of the two beams, helping to ensure a deep null. Other elements in the system include shutters for alignment and calibration purposes, an assembly for amplitude control of the fringe null, and optical fibers for wavefront cleanup. The fibers help achieve the desired null depth with reduced tolerances on the preceding optical components (in order to reduce manufacturing costs). The dark and bright outputs are sent to their respective Focal Plane Arrays (FPAs) that are long wavelength HgCdTe arrays from Teledyne (previously Rockwell) operating at 35K. The FPAs for the fringe and angle trackers are operated at 77K and are based on the HgCdTe NICMOS arrays. Cryogenic delay lines are used to equalize the pathlengths between the two sides of the interferometer.

When the instrument is in operation, it rotates slowly around the line of sight to the object. In doing so, a sinusoidal signal is generated at the output of the nuller instrument, which is non-zero if there is a planet or material within the transmission pattern of the nuller. Data from the bright port is also taken providing measurements of the visibility of the object. Simulations have been performed, both for nulling operation as well as imaging (Danchi et al. 2003a; Barry et al. 2005, 2006).

	A - Design	B - Design	C - Design
Key Requirements			
Mission Life (on station)	5 years (science operations)	1 year (science operations)	2 years (science operations)
Science Capability	Imaging, Nulling	Imaging, Nulling	Nulling
Science Wavelength Range	5.0 - 28.0 microns	5.0 - 28.0 microns	3.0 - 8.0 microns
Science Viewing Angle	+/- 20 deg off ecliptic	+/- 10 deg off ecliptic	+/- 18.5 deg off ecliptic +/- 7.5 deg within ecliptic
Observing Rotation Rate	1 rev/hr (max)	0.5 rev/hr (max)	2 rev/hr (max)
Science Data Collect Rate	148 Gb/day (normal mode)	61 Gb/day (normal mode)	1.1 Gb/day (normal w/o margin)
Instr. Thermal Stability	1K/day	1K/day	1K/day
Science Detector Temp	6K (max)	6K (max)	35K (max)
Near IR Detector Temps	30K (max)	77K (max)	77K (max)
Phase B Start to Launch	54 months (no margin)	46 months (no margin)	61 months (incl. 6 mo. margin)
Key Configuration Aspects			
Science Telescopes	5	3	2 (mounted inboard)
Instrument Elements	AT, FT, FTS, (Nuller)	AT, FT, R=10,000 FTS, (Nuller)	AT, FT, Nuller, R = 20 max dispersive element
Interferometer Type	Fizeau (image plane)	Fizeau (image plane)	Michelson (pupil plane)
Boresight Separation	20 m (four -fold boom)	16 m (four -fold boom)	12.5 m (two -fold boom)
Cryocooling	Two 6K ACTD coolers (Low TRL) & (4) 40K coolers	6K cryostat (H ₂ Dewar) + (2) 30K coolers (IM/near IR detect)	One 32K cooler, near IR detectors passively cooled
Sunshield Location	On Bus	On Bus	On Instrument Boom
Propulsion System	Hydrazine / He Cold Gas	All Hydrazine	All Hydrazine
ACS	6 wheel (Rx + momentum)	Com'l, 4 small Rx wheels	Com'l, 4 medium Rx wheels
Star Trackers	6 Total (4 on instr., 2 on bus)	2 (on bus)	2 (on bus - instr. attitude info passed to bus)
Slew Rate (peak)	0.67 deg/min	0.33 deg/min	Up to 6.1 deg/ min (w/3 wheels)
High Gain Antenna Type	2-axis gimbal	Fixed	2-axis gimbal
Ground Contacts	Every 1.0 day (DSN)	Every 1.5 days (DSN)	2x per day (com'l stations)
Instrument Plan/Schedule	Done by Mission Ops Team	Done by Instrument team	Done by Instrument team
Mass, Wet w/contin. (kg)	3,710	3,083	3,183
Power, EOL w/contin. (W)	1,448	1,029	766
Fairing Diameter (m)	5	5	4

Figure 8. Trade parameter space for Designs A, B, and C. Design A allows for a complete system of 5 telescopes with both nulling planet detection and wide-field high angular resolution imaging from 5-28 μm . Design B is an austere design, but it retains 3 telescopes and a capability for imaging but only with a single closure phase. Design C emphasizes nulling with 2 telescopes from 3-8 μm . This is the FKSII baseline design (see Danchi et al. 2003b).

The concept discussed above has undergone a thorough integrated analysis and modeling study of the structure and optics to validate the design and ensure that it meets requirements (Hyde et al. 2004). A major concern was the propagation of reaction-wheel disturbances from the spacecraft bus through the bus-instrument package coupling up to the boom system. The null depth requirement was shown to drive the instrument performance. The allocation of 6 nm for high frequency jitter from the reaction wheels was included. Other sources of noise include the Fringe Tracker (FT), the Optical Delay Line (ODL), the Attitude Control System (ACS), and the booms themselves. The boom system had lowest order modes at 5.6 and 7.3 Hz. A substantial safety margin of 9.4 nm was also allocated. Through this modeling

and validation campaign, the closed loop performance requirement could be met or exceeded at all wheel speeds from 0.1 to 100 Hz.

5. PERFORMANCE

Figure 3 (left panel) displays a table of planetary characteristics and what can be determined using a modest nulling interferometer, such as planetary temperature, radius, mass density, albedo, surface gravity, and atmospheric composition, including the presence of water. To date, progress has been made on the physical characteristics of planets largely through transiting systems, but a small planet finding interferometer can measure the emission spectra of a large number of the non-transiting ones, as well as more precise spectra of the transiting ones.

Many molecular species, such as carbon monoxide, methane, and water vapor, have strong spectral features in the 3-8 μm region, as can be seen in Figure 3 (right panel), which displays model atmospheres for extrasolar planets calculated by Seager (2005), for planets at various distances from the host star. The red curve shows the theoretical spectrum of a very hot, close-in planet at 0.05 AU, while the blue curve displays spectrum for a much cooler planet ten times further out, at 0.5 AU. Also displayed are sensitivity curves for the IRAC instrument on Spitzer (light blue) and FKSI (purple). Clearly such a mission concept has sufficient sensitivity to detect and characterize a broad range of extrasolar planets.

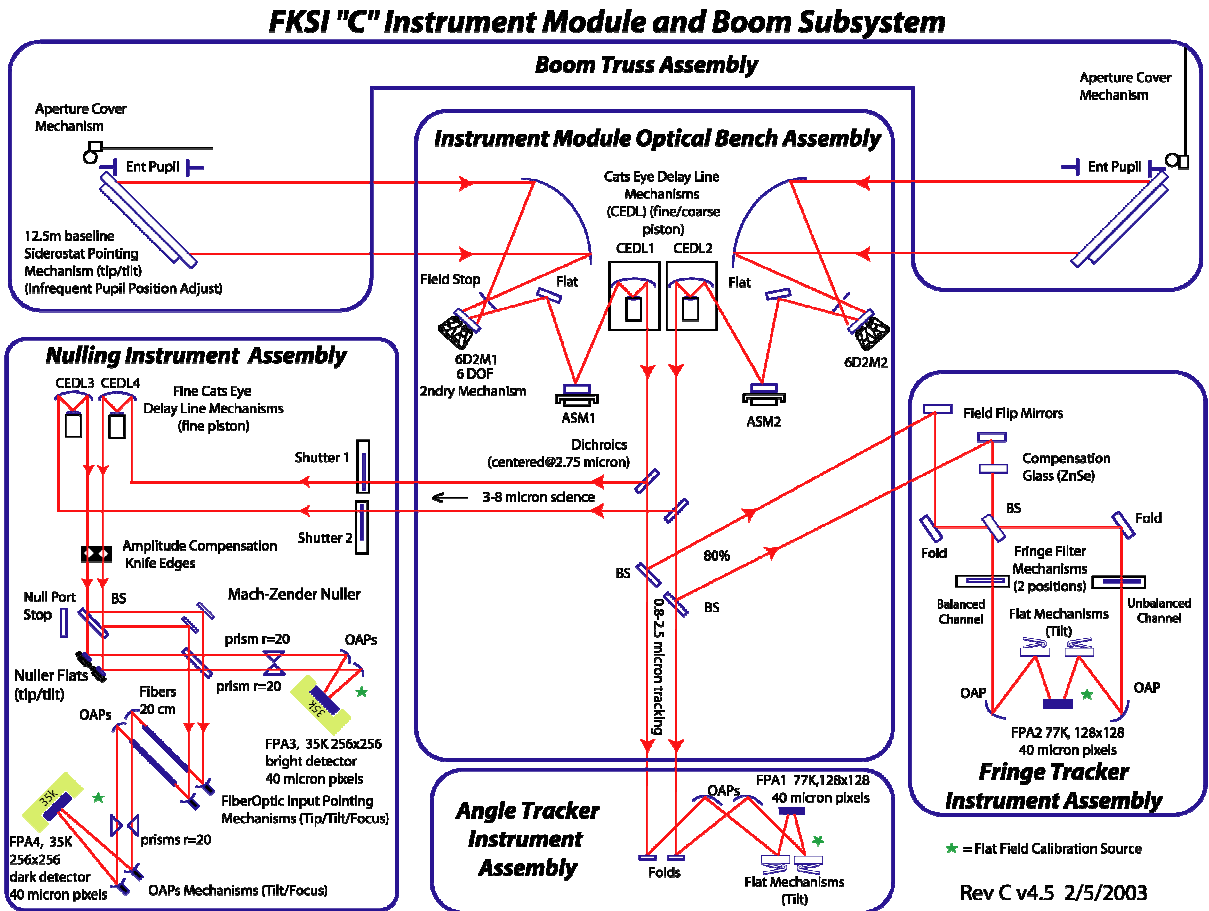


Figure 9. Schematic design of the boom and instrument module subsystem for FKSI. The various subassemblies are as noted in the figure.

Initial studies with very conservative assumptions of an 8 m boom length, 140 extrasolar planets (known at that time), 120 second on-source integration time, 15 nm rms path length error, telescope temperature of 65K, and a small sunshield with a ± 20 degree field of regard; gave ~ 25 detections (Barry et al. 2006). Currently, there are about 250 known planets, so with those assumptions and the same detection ratio of about 18%, we expect to be able to detect and

characterize about 45 exoplanets, and a larger sunshade with a field of regard of ± 45 degrees, would approximately double this number to ~ 90 planets.

Recent studies of the detectability of debris disks (Defrere et al. 2008) demonstrated that the residual pathlength error for a small system like FKSI should be of the order of 2 nm rms, which would significantly increase the number. As a conservative estimate, we expect that a small system could detect (e.g. remove the $\sin(i)$ ambiguity) and characterize about 75-100 known exoplanets.

These recent studies also have shown that a small mission is ideal for the detection and characterization of exozodiacal and debris disks around *ALL TPF candidate stars* in the Solar neighborhood as seen in Figures 10 and 11. (Defrere et al. 2008). Indeed, the performance level of the FKSI system is of the order of 1 Solar System Zodi (SSZ) in 30 minutes of integration for a G0 star at 30 pc. With a small sunshade this system could observe of the order of 450 stars in the Solar neighborhood, and with a larger field-of-regard, such as ± 45 degrees, the exozodiacal dust and debris disks of about 1000 stars could be studied.

Recently, Wallner et al. (2008) have shown that knowledge of the exozodiacal dust emission level to 1 SSZ is important in planning future flagship missions as this knowledge affects the strategy for the spectroscopic measurements of atmospheres of earth-sized planets. **Thus both knowledge of which stars have earth-sized planets (astrometric and and perhaps RV measurements) and those that have low exozodi levels (FKSI) is vital to the formulation and strategy of the flagship TPF and Darwin missions.**

If the telescopes are somewhat larger than has been discussed in some of the existing mission concepts (e.g., 1-2 m) and are somewhat cooler (e.g., $< 60\text{K}$) so that the system can operate at longer wavelengths, it is possible for a small infrared structurally-connected interferometer to detect and characterize super-earths and even $\sim 50\text{-}75$ earth-sized planets around the nearest stars. This is especially important now that there is evidence that lower mass planets are very common, based on the detection of the 5.5 Earth mass planet using the microlensing approach (e.g. Beaulieu et al. 2006, Gould et al. 2006).

Further studies of the capabilities of a small infrared structurally-connected interferometer are necessary to improve upon our estimates of system performance.

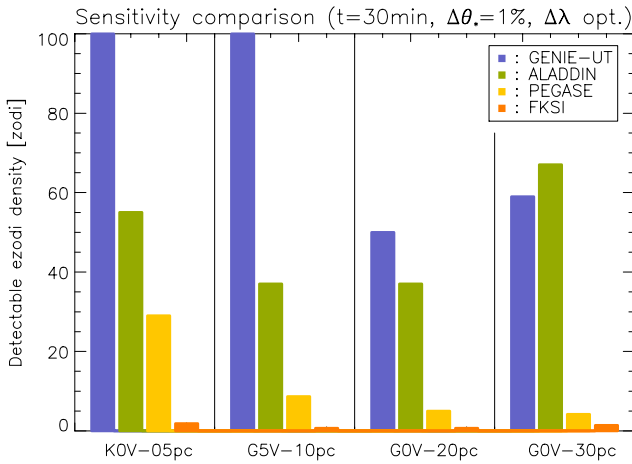


Figure 10. Expected performance for Pegase and FKSI compared to the ground-based instruments (for 30 min integration time and 1% uncertainty on the stellar angular diameters).

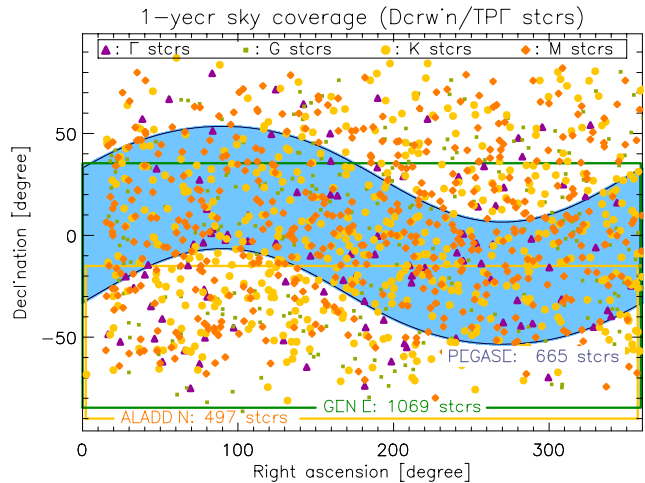


Figure 11. Sky coverage after 1 year of observation of GENIE (dark frame), ALADDIN (light frame) and Pegase (shaded area) shown with the Darwin/TPF all sky target catalogue. The blue-shaded area shows the sky coverage of a space-based instrument with an ecliptic latitude in the $[-30^\circ, 30^\circ]$ range (such as Pegase). The sky coverage of FKSI is similar to that of Pegase with an extension of 40° instead of 60° .

6. TECHNOLOGY PROGRESS AND TECHNICAL READINESS LEVELS

Table 1 displays a summary of the technical readiness levels (TRLs) of key technologies used in the small infrared structurally connected interferometer (FKSI) mission. These levels are estimated using NASA standard terminology for them (Mankins 1995).

Many of the key technological hurdles for FKSI as understood in the original studies performed by our group in 2002-2003 have been solved by NASA flagships projects, in particular, the investments in JWST and TPF-I/Darwin technologies can be directly used in the FKSI system. As of early 2007, JWST passed all of its key technology milestones, including those for cryocoolers, precision cryogenic support structures, detectors, cryogenic mirrors, and sunshades. All of these technologies are ready for implementation in the FKSI mission.

Table 1. Technical Readiness Levels for Key Subsystem Components

Item	Description	TRL	Notes
1	Cryocoolers	6	Source: JWST
2	Precision cryogenic structure (booms)	6	Source: JWST
3	Detectors (near-infrared)	6	Source: HST, JWST Nircam
4	Detectors (mid-infrared)	6	Source: Spitzer IRAC, JWST MIRI
5	Cryogenic mirrors	6	Source: JWST
6	Optical fiber for mid-infrared	4	Source: TPF-I
7	Sunshade	6	Source: JWST
8	Nuller Instrument	5	Source: Keck Interferometer Nuller, TPF-I project, LBTI
9	Precision cryogenic delay line	6	Source: ESA Darwin

*Note: The requirement for the FKSI project is a null depth of 10^{-4} in a 10% bandwidth. Laboratory results with the TPF-I testbeds have exceeded this requirement by an order of magnitude (Lawson et al. 2008).

Key technologies unique to the FKSI mission have also benefited from NASA's investments in the Keck Interferometer Nuller system (now in operation at the Keck Observatory) and the TPF-I testbeds at JPL including the Planet Detection Testbed and the Adaptive Nuller (Lawson et al. 2008). The demonstrated broadband null depths from these testbeds approach 1×10^{-5} , about an order of magnitude better than the requirements for the FKSI mission (Peters et al. 2008).

The optical fibers needed for wavefront cleanup have been fabricated and tested at room temperature as part of the TPF-I technology program. Currently two types of fibers have been tested in the laboratory and work sufficiently well for the FKSI mission, these are chalcogenide fibers fabricated at the Naval Research Laboratory (NRL) (Aggarwal & Sanghera 2002; Ksendzov et al. 2007) that operate from the near- to mid-infrared, and silver halide fibers developed at Tel Aviv University that operate in the longer wavelength part of the mid-infrared (see Ksendzov et al. 2008; Lewi et al. 2008 and references therein). A third type of fiber, a hollow glass waveguide fiber developed at Rutgers University (Harrington 2001) may also be of use. Further testing is planned, including cryogenic testing of all fibers.

At a system level, a nuller instrument fabricated at JPL has been delivered to and is in use at the Keck Observatory. The FKSI nuller instrument is actually simpler than the Keck instrument, as the latter requires chopping out the background created by a warm telescope and sky (not needed by FKSI). Indeed the first data from the Keck Interferometer Nuller has recently been published (Barry et al. 2008). The Bracewell Infrared Nulling Cryostat (BLINC, Hinz et al. 2000) is a cryogenic nuller in use on the MMT, which has achieved significant results in studies of accretion disks around Herbig Ae/Be stars.

Finally, FKSI requires a precision cryogenic delay line with a stroke of the order of a centimeter. TNO, a commercial firm in Europe, under contract from ESA has developed such a prototype cryogenic delay line, which is at a high TRL level. This delay line has a precision of <1.3 nm and a stroke of 20 mm, which is more than adequate for a small interferometer. Also three cryogenic delay lines have been flown as part of three Michelson (Fourier Transform Spectrometers) spectral interferometers, and of them, two were developed at the Goddard Space Flight Center. One was the FIRAS instrument on the COBE mission, which won a Nobel Prize in Physics for Drs. J. Mather and G. Smoot for cosmic microwave background research (Mather et al. 1994). A second has been flown successfully on the CASSINI

mission, for the CIRES instrument¹. A third delay line is on the Atmospheric Chemistry Experiment-Fourier Transform Spectrometer (ACE-FTS) – Canada’s Earth Science Interferometer on board the Canadian satellite SCISAT-1, captures spectra and images used to investigate chemical and dynamical processes in Earth’s atmosphere, with a particular emphasis on ozone depletion in the Arctic stratosphere².

In summary, we note only one area where technology development is needed for a Phase A start for a small infrared structurally-connected interferometer, which is cryogenic testing of the optical fibers for wavefront cleanup.

7. COST/SCIENCE RETURN TRADES

Recent discussions from NASA Headquarters indicate that a possible “Exoplanet Probe” funding line may open up in the next few years depending on NASA’s budgetary situation and Congressional approval. The current design for the FKSI mission is based on work performed a few years ago in preparation for a Discovery Announcement of Opportunity (AO), which at that time had a cost cap, including launch vehicle, of \$425 M. The FKSI budget was somewhat above that and for that reason it was not proposed during that particular round. However, scientific and technological progress has been such that FKSI is widely regarded as a viable pathfinding mission for the flagship class TPF-I and Darwin that is ready for a Phase A start as soon as the Exoplanet Probe line is funded. The total cost estimate as of December 2007, in FY2008 dollars was just above \$600M, including launch vehicle and generous margins (30%) for all cost elements in the Work Breakdown Structure (WBS), except for the launch vehicle, which had a 10% margin (Danchi et al. 2007, unpublished ACMCS proposal). Our present understanding is that the cost cap for an Exoplanet Probe mission will be \$600 M in FY08 dollars, without the launch vehicle, which is to be provided separately by NASA Headquarters. The budgeted amount for the launch vehicle for FKSI was \$160 M for the smallest Atlas V rocket with a 4-m diameter fairing. Thus, given the \$600 M cost cap, FKSI is presently well under the cap, leaving approximately \$180 M for science and cost trades, which are well worth investigating. In addition, there may be cost savings due to technology re-use and perhaps even hardware re-use from the JWST project, which for example, has developed detector, cryocooler, sunshade, large optics, and other technologies which are immediately useful to the FKSI mission.

Hence for the purpose of discussion, we list some possible trades that would be of use to further develop the mission concept for the anticipated Announcement of Opportunity for the Exoplanet Probe line. The list in Table 2 is self-explanatory, and we make only few comments here to provide some context for the discussion in the table. Perhaps the most significant trades are related to the wavelength range and temperature of the telescopes and structure. Part of the Discovery studies led us to reduce the wavelength range from 5-20 μm to 3-8 μm , which allowed a greatly simplified sunshade, and a reduced requirement for passive cooling from 35-40 K to 60-65 K. However, even at 60 K the local zodiacal cloud dominates the noise up to wavelengths of about 10 μm or so. Hence, a first trade would be to extend the Field-of-Regard for the sunshade from ± 20 degrees to ± 45 degrees, which doubles the science return given that a much larger area of the sky can be probed. A second trade would be to understand the cost implications of a sunshade that would allow us to extend the wavelength range to better match what is desired for TPF-I and Darwin, allowing for studies of cooler material and more sensitivity to Super-Earth and Earth-sized planets in the habitable zone. This trade has to be evaluated against the other option, which is to keep everything the same as before, but simply to put in larger apertures to 1-1.3 m class, which also significantly improves the sensitivity. The other trades which are most crucial are related to cryocooler and detector technologies, which could be directly borrowed from JWST, rather than following our original plan, based on HST cryocoolers and long wavelength HgCdTe detectors, which have not progressed as far technologically, not because these are hard to do, but because of the much more substantial investments to JWST. The final most important trade would be adding a third telescope and increasing the maximum baseline to 20 meters. All of these trade studies could be done in less than one year providing funding was available to the science and technology teams.

¹ <http://saturn.jpl.nasa.gov/spacecraft/inst-cassini-cirs-details.cfm>

² <http://www.ace.uwaterloo.ca/>

Table 2. Science/Cost Trades

Item	Discussion
1.1 Detectors	New options exist for the science detectors. Our previous choice was a long-wavelength version of HgCdTe detectors used on NICMOS and JWST. These detectors operate from 3 to 8 μm , but are at a lower TRL than mid-infrared detectors for MIRI, which can also operate in this wavelength range. Si:As detectors with short wavelength optimization could also work for FKSI, but these detectors need to be operated at 7 K, instead of 35 K, as are needed for the HgCdTe detectors. Thus the cost of bringing up the TRL level of the HgCdTe detectors needs to be balanced against the cost of a more complex cryogenic system.
1.2 Cryocoolers.	The original choice for cryocoolers for FKSI was based on those used on HST that operate at 77K for the NICMOS detectors. These could be adapted for a colder operating temperature (35 K). However, apart from the detector issue noted above, it is also possible to directly utilize the JWST cryocoolers from MIRI, regardless of which detector is ultimately chosen. Alternatively, if long-wavelength HgCdTe detectors are used, then it may be possible to eliminate cryocoolers altogether by utilizing radiators on the top of the booms and cryopumped loops.
2.1 Large Optics	The present design is based on 0.5 m optics from light-weighted aluminum. Advances in technology from JWST with beryllium optics means that perhaps 1-m diameter optics can be used, which could provide improved capabilities at lower total mass than before.
2.2 Architecture.	Investigate whether the increased budget allowed within the mid-cost price range would allow for 3 telescopes instead of 2 as is currently planned. This would significantly increase the capability of the mission.
2.3 Sunshade Design	The baseline design has a fixed sunshade with a ± 20 degree field of regard with respect to the anti-sun direction. It is highly desirable to have one with ± 45 degrees, which could be a simple deployable one attached to the fixed sunshade. This possibility had been discussed in the past, and needs to be re-examined in the proposed study.
2.4 Integration and Testing	The FKSI mission has a well-developed test plan, however, it needs to be updated based on the proposed study. Also the overall final full system test potentially could be performed in the large test chamber at Marshall Space Flight Center without the use of “stub” booms that were designed for testing in the largest chamber at Goddard.
3.1 Fiber Optics	Chalcogenide and silver halide single mode fibers have been developed for TPF-I and Darwin. It would be interesting to examine hollow glass waveguides as well, and develop a technology plan for these fibers in particular, to see if they are viable. All fibers need to be tested in cryogenic conditions in order to bring them up to a TRL sufficient for Phase A.
3.2 Nuller Instrument.	The present design uses a modified Mach-Zehnder beamsplitter arrangement. It would be useful to investigate whether a simpler design using only a single optimized beamsplitter could achieve the required null depth, also to investigate whether any technologies from the BLINC instrument can be used on the FKSI nuller.
3.3 Fringe tracking system	Currently this subsystem is separated from the Nuller Instrument, which means there could be non-common path errors affecting the Nuller Instrument that are now compensated for by low-bandwidth, short stroke delay lines on the nuller instrument itself. It is worthwhile to investigate whether this subsystem can be incorporated within the Nulling Instrument, possibly saving on mass, cost, complexity. The LBTI has an integrated fringe tracking system, which may be applicable to FKSI. We may be able to use the LBTI design as a baseline for this part of the study.

4.1 Design Reference Mission	Perform a study of sample observations for key projects for FCSI and use this information to re-examine mission and science operations scenarios. Also investigate broader science opportunities that do not significantly impact on costs, but enhance the mission overall
5.1 Cost estimation	Revise cost estimate based on the above modifications to the baseline design and changes in the mass budget, as well as greater understanding of costs based on JWST

8. SUMMARY AND CONCLUSIONS

The FCSI mission concept is a well-studied, and scientifically and technologically viable, Exoplanet Probe class mission that could lead us within the next decade to the characterization of our nearest Earth twins. Given the broad scientific and cultural impact of such discoveries we believe that continued investments towards the direct detection and characterization of exoplanets in the infrared is an important and worthy goal for space astronomy in the next decade.

9. ACKNOWLEDGMENTS

The research described in this paper was carried out at NASA's Goddard Space Flight Center and at the Jet Propulsion Laboratory, California Institute of Technology, the latter under a contract with the National Aeronautics and Space Administration.

REFERENCES

- [1] Aggarwal, I.D. & Sanghera, J.S. 2002, *J. Optoelectron. Adv. Mater* 4, 665.
- [2] Alonso, et al. 2004, *ApJ*, 613, L153.
- [3] Auman et al. 1984, *ApJ*, 278, L23.
- [4] Barry, R. et al. 2005, *Proc. SPIE*, 5905, 311.
- [5] Barry, R. et al. 2006a, *Proc. SPIE*, 6265.
- [6] Barry, R. et al. 2006b, *IAU Colloq. 200: Direct Imaging of Exoplanets: Science and Techniques*, 185.
- [7] Barry et al. 2008a, in *The Power of Optical/IR Interferometry: Recent Scientific Results and 2nd Generation Instruments*, 547.
- [8] Barry, R. et al. 2008b, *ApJ*, XXX, XXX.
- [9] Beichman et al. 2005, *ApJ*, 622, 1160.
- [10] Beaulieu, J.-P. et al. 2006, *Nature*, 439, 437.
- [11] Bryden, G. et al. 2006, *ApJ*, 636, 1098.
- [12] Bennett, D.P. et al. 1999, *Nature*, 402, 57.
- [13] Charbonneau, D. et al. 1999, *ApJ*, 529, 45.
- [14] Charbonneau, D. et al. 2002, *ApJ*, 568, 377.
- [15] Charbonneau, D. et al. 2005, *ApJ*, 626, 523.
- [16] Chauvin, G. et al. 2005, *A&A*, 438L, 25.
- [17] Danchi et al. 2003a, *ApJ*, 597L, 570.
- [18] Danchi, W.C. et al. 2003b, *Proc. Conf. on Towards Other Earths*, ESA SP-539.
- [19] Danchi et al. 2004, *Proc. SPIE*, 5491, 236.
- [20] Danchi, W., et al. 2006, *Proc. SPIE*, 6268, XX.
- [21] Danchi, W., Lopez, B. 2007, *Comptes Rendus Physique*, 8, 396.
- [22] Defrere, D. Absil, O., Hanot, C., and Fridlund, M. 2007, *Proc. SPIE*, 6693, 53.
- [23] Defrere, D., Absil, O., V. Foresto, W. C. Danchi, R.den Hartog, 2008, submitted to *A&A*.
- [24] Deming, D. et al. 2005, *Nature*, 434, 740.
- [25] Deming, D. et al. 2006, *ApJ*, 644, 560.
- [26] Dermott et al. 2002, in *Asteroids III* (Tucson: Univ. of Arizona Press), 423.
- [27] Duigou et al. 2006, *Proc. SPIE*, 6265
- [28] Frey, B. et al. 2006, *Proc. SPIE*, 6265.
- [29] Gaudi et al. 2005, *ApJ*, 628, 73.
- [30] Gould, A. et al. 2006, *ApJ*, 644, L37.
- [31] Greaves et al. 1998, *ApJ*, 506, 133.
- [32] Greaves et al. 2004, *MNRAS*, 348, 1097.
- [33] Grillmair, X., et al. 2007, 658, L115.
- [34] Guillot, T., & Showman, A.P. 2002, *A&A*, 385, 156
- [35] Harrington, J. A. 2001, *Infrared Fiber Optics*, M. Bass, J. Enoch, E. Van Stryland, and W. Wolfe, eds., (McGraw-Hill, New York).
- [36] Hinz, P.M. et al. 2000, *Proc. SPIE* 4006, 349.
- [37] Hinz, P.M. et al. 2006, *ApJ* 653, 1486.
- [38] Holland, W. et al. 2003, *ApJ*, 582, 1146.
- [39] Holland, W. et al. 1998, *Nature*, 392, 788.
- [40] Hyde T.T., et al. 2004, *Proc. SPIE*, 5497, 553.
- [41] Jayawardhana et al. 1998, *ApJ*, 503, L79.
- [42] Harrington, J. 1997,
- [43] Koerner et al. 1998. *ApJ*, 503, L83.
- [44] Kszendzov, A. et al. 2007, *Appl. Opt.*, 46, 7957.

- [45] Ksendzov, A. et al. 2008, Appl. Opt., 47, submitted.
- [46] Kim et al. 2005, ApJ, 632, 659.
- [47] Lafreniere, D. et al. 2007, ApJ accepted.
- [48] Lawson, P. R. et al. 2008, Proc. SPIE, 7013.
- [49] Lewi, T. et al. 2008, Proc. SPIE 7013.
- [50] Lissauer, J. & DePater, I. 2001, "*Planetary Sciences*," [Cambridge, UK: Cambridge University Press].
- [51] Lunine, J. 2001, PNAS 98, 809.
- [52] Lunine, J. et al. 2008, report from the ExoPlanet Task Force, <http://www.nsf.gov/mps/ast/exoptf.jsp>.
- [53] Mankins 1995, NASA white paper on Technical Readiness Levels, unpublished.
- [54] Marriotti, J.M. & Ridgway, S. 1988, A&A, 195, 350.
- [55] Mather, J. et al. 1994, ApJ, 420, 439.
- [56] Mayor, M., & Queloz, D. 1995, Nature, 378, 55.
- [57] Marcy, G.W., & Butler, P. 1998, ARAA, 36, 57.
- [58] Peters, R. D. et al. 2008, Appl Opt. 47, in press.
- [59] Plets, H. & Vynckier, C. 1999, A&A, 343, 496.
- [60] Reach et al. 2003, Icarus, 164, 384.
- [61] Reach et al. 2005, ApJ, 635, L161.
- [62] Reike et al. 2005, ApJ, 620, 1010.
- [63] Richardson, L.J. et al. 2006, IAU Colloquium 200: Direct Imaging of Exoplanets: Science and Techniques, 185.
- [64] Richardson, L.J. et al. 2007, Nature, 445, 892.
- [65] Rowe, J.P. et al. 2006, arXiv:astro-ph, 0603410.
- [66] Seager, S. 2005, private communication.
- [67] Schneider, J. 2008, <http://exoplanet.eu>.
- [68] Showman & Guillot 2002, A&A, 385, 156.
- [69] Spangler, C. et al. 2001, ApJ, 555, 932.
- [70] Selsis, F. et al. 2007, A&A accepted.
- [71] Stern, S.A. 1996, A&A, 310, 999.
- [72] Vidal-Madjar, et al. 2003, Nature, 422, 143.
- [73] Wallner, O. et al., Proc. SPIE, 7013, this conference.
- [74] Wolszczan, A., & Frail, D. 1992, Nature, 355, 145